//4

JOURNAL

OF

GEOMAGNETISM

AND

GEOELECTRICITY

VOL. 1. NO. 1.

SOCIETY

OF

TERRESTRIAL MAGNETISM AND ELECTRICITY

March 1949

KYOTO

JOURNAL OF GEOMAGNETISM AND GEOELECTRICITY

The fields of interest of this quarterly Journal are as follows:

Terrestrial Magnetism	Aurora and Night Sky
Atmospheric Electricity	The Ozone Layer
The Ionosphere	Physical States of the Upper Atmosphere
Radio Wave Propagation	Solar Phenomena Relating to the Above Subjects
Cosmic Rays	Electricity within the Earth

The text should be written in English, German or French. The price is provisionally set as 180 yen per copy subject to change. We hope to exchange this Journal with periodical publications of any kind in the field of natural science.

The editor.

EDITORIAL OFFICE: Society of Terrestrial Magnetism and Electricity,
Kyoto University, Japan

EDITORIAL SECRETARIES: M. Ota and S. Matsushita
(Kyoto Uuiversity)

Some Application of Modern Mathematical Statistic to the Lunar Tidal Analysis of Ionospheric Height.

By K. MAEDA and M. IZAKI

(Electrical Communication Laboratory, Ministry of Telecommunications.)

Summary

The paper deals with some problems of lunnar tidal anlyses of ionospheric height, which are treated from the standpoint of mathematical statistics. The semi-amplitude of lunar semi-diurnal tide of Z_mF_2 (height of maximum electron density of F_2 region) analyzed from Japanese data is tested by statistical hypothesis and its results are described. Next the error caused by a rough scaling of height is estimated in connection to scaler's skill (or carefulness), and the results are given.

Some statistical measures are introduced for the criterion of the validity of analyzed results in the above treatments, that is, the level of significrnce for the former case (test of statistical hypothesis by non-parametric method) and the coefficient of confidence for the later case (estimation of error).

I. Introduction

(with particular reference to the work by Chapman and Bartels)[1]

The movements in the ionosphere, such as wind, circulation, tidal motions etc., have recently been considered as one of the most importants problems of the ionosphere physics. The lunar tidal phenomena of the ionospheric height have been revealed by many scientists on the basis of various analyses of observed results and it is reported that amplitude of the semi-diurnal lunar tide of the ionospheric height will be a few kilometers.

In the harmonic analyses of ionospheric data careful considerations should be paid to the observed materials themselves, their selection and arrangement for analyses and the method of analysis, and fairly elaborate works are necessary to evaluate the errors and to test the periodicities. Regarding these problems we can find and extensive study in "Geomagnetism" vol. II. by S. Chapman and J. Bartels.[1] Although this book covers every item of importance for the harmonic analysis, it shall not be unnecessary to treat a few problems of analyses on the basis of modern mathematico-statistical conception, the methods by which will be briefly described in contrast to those written in Geomagnetism.

In this book the investigation of periodicity is discussed (§30 in p. 593 and equation (86) in §25), but it is necessary to know a parameter in population, that is the variance, which is put approximately equal to the sample variance in the case of a great number of data. The present authors made the test of statistical hypothesis by using the non-parametric method, such as F-distribution.

Also in the book (p. 581 and others) the effect of observation errors is discussed, and we will discuss the effect of scale in connection to scaling skill (or carefulness), which is different from that described in the book.

Before making the harmonic analysis, or applying the test of statistical hypothesis on periodicities and estimating the errors, it is necessary to make the process stationary (for example, to eliminate trends) and to investigate the elements, which construct the process in population (to make the correlogram), and finally to perform the test of statistical hypothesis on these investigations. The quasi-persistence introduced in the book corresponds to the trends and several persistence curves (Fig. 12 p. 589) involve the same sense as the correlogram. But these investigations will become complete after the test of statistical hypothesis on themselves.

The problems of stationary process and correlogram are not described here in detail, but we want to point out here some problems from the consideration of the current observational practice of the ionosphere and to discuss some of them statistically in the following sections.

Problem 1. Even if we can measure the ionospheric height in a sufficient accuracy (i. e. height mark of sufficiently small step) and on lunar time basis (i. e. lunar hourly or semi-hourly base), it is necessary to test the significance of the analyzed result statistically, as sampling errors are involved.

Problem 2. The scaling practice of the ionospheric height of current use in the world is 10 Km step. Such quantization of the height record is comparatively great and is seriously connected to the validity of the analyzed results. In this case the skill (or carefulness) of scalers should be taken into account.

The problem is restated as follows. How long should be the period for the analysis (a month, a season or a year), or how much should be the number of observed materials for the analysis, in order to obtain sufficiently small errors in connection to the quantization of scaling skill (or carefulness)?

Problem 3. In most cases of the lunar tidal analyses we have to use data observed on solar time basis and the difference of time basis (solar and lunar) will exert errors to the analyzed results.

In the first problem(2) we can apply the test of statistical hypothesis by non-parametric method and obtain a definite level of significance for each individual result of analysis. In rhe second problem we can determine an average error with a certain definite coefficient of confidence for each individual results analyzed from a certain number of observed values (sample size).

In the following the writers describe some typical examples of the above two problems, which are treated in the light of mathematical statistics. The third problem

is left for the future study.

II. Errors and distributions of observed values.

Ionospheric data of Japan were analyzed by Matsushita and it was reported by him[3] that the semi-amplitude of a half-day period (lunar-time) of Z_mF_2 (height of maximum electron density of F_2 region) was about 3 Km. In his analysis the errors caused by fixing a reading scale of the ionospheric height at 10 Km step and by the difference between lunar and solar time bases are involved. Even in cases of accurate measurements performed with a sufficiently precise reading and on lunar hourly base, sampling errors will be involved so far as the materials for the analyses are observed data. Therefore the test of statistical hypothesis or the statistical estimation must be carried out in order to account the obtained value (such as 3 Km) as the real effect of tidal movement.

Before the harmonic analysis on observed data is performed, the several steps which are described in the preceding section (to make the process stationary and to investigate the process by making correlogram etc.) must be taken, but the description on these points is omitted here, and we assume that the necessary data $u(t)$ for harmonic analysis is the sum of errors $\delta(t)$ due to height scaling practice and $x(t)$ which should correspond to the phenomena represented by the equation as follows.

$$x(t)=\sum_{r=1}^{h}(a_r\cos\lambda_r t+b_r\sin\lambda_r t)+v(t)=\sum_{r=1}^{h}c_r\cos(\lambda_r t+\varphi_r)+v(t)=m(t)+v(t) \qquad (1)$$

$v(t)$ is a random element and there will be no objection in taking it as Gaussian distribution $N(o,\sigma^2)$ in our case. Also we assume here that the material can be arranged so as every solar cyclic term is eliminated.

Thus, we obtain as the equation of abserved value $u(t)$,

$$u(t)=x(t)+\delta(t)=m(t)+v(t)+\delta(t)$$

and this will show a discrete distribution with the minimum interval of the height mark (say 10 Km). In any case the observed value is more or less discrete. The discreteness will not be the problem, but the point is the relative comparison between the minimum unit of height scale and the state of distribution (here, σ^2). In our case, it seems that the scale is fairly rough to take $u(t)$ as continuous, judging from the distribution of $u(t)$. Even if we can take as continuous, it deviates more or less from the Gaussian distribution owing to the errors (δ) of scaling.

But considering from the practical aspect, it will be better that we first put $u(t)$ as $N(m(t),\sigma^2)$ and estimate the level of significance in the test of statistical hypothesis as discribed in the following section, and after that we take the actual level as a little higher than the level based on normol distribution.

III. Significance of Harmonic Analysis

We put the observed value $u(t)$ as $N(m(t),\sigma^2)$ tentatively, considering the discussions in the preceding section.

Then the equation

$$F=\frac{\frac{1}{2}[(\hat{a}_r-a_r)^2+(\hat{b}_r-b_r)^2]}{2} \bigg/ \frac{\frac{1}{N}\sum_{t=1}^{N}u_t^2-\left(\frac{1}{N}\sum_{t=1}^{N}u_t\right)^2-\frac{1}{2}\sum_{r=1}^{h}(\hat{a}_r^2+\hat{b}_r^2)}{N-2h-1} \tag{2}$$

where $\hat{a}_r=\frac{2}{N}\sum u(t)\cos\lambda_r t,\quad \hat{b}_r=\frac{2}{N}\sum u(t)\sin\lambda_r t$

$\lambda_r=2\pi\frac{r}{24}\qquad r=1, 2, \ldots, h)$

indicates the F-distribution with the degrees of freedom $(2, N-2h-1)$ based on the normal regression theory*. In equation (2) N is a number of observed data, and $\sum$ working on u_t and u_t^2 is the sum of all data, and $\sum$ of the last term in the denominator is the sum covering every semi-amplitude calculated for a definite number (h) of lunar harmonics that were supposed to exist a priori. By giving suitable values to a_r and b_r in the numerator of equation (2), we can perform a test of statistical hypothesis on the semi-amplitude under consideration. It is worthy of notice that in this equation (2) no parameters in population are involved.

Here we employ the method of null-hypothesis, that is, we calculate the equation (2) by putting $c_r=0$ $(a_r=0,\ b_r=0)$. The value of F of equation (2) for this case can be calculated from the data and we put it as F_0.

On the other hand from the table already made, we know values of $F^2_{N-2h-1}(\alpha)$ with the degrees of freedom 2 and $N-2h-1$ and for the level of significance α. And in the case when

$$F_0>F^2_{N-2h-1}(\alpha) \tag{3}$$

we must reject the hypothesis $c_r=0$ with the significance level α. Therefore it can be mentioned that c_r is significant, but this mention may not be right with the rate of α.

In the following we apply the test of statistical hypothesis on some of the results of half-day period (lunar time) in the harmonic analysis worked out by Matsushita.

The following table I shows three examples reported by Matsushita.

Table I

Period	semi-amp. (Km) I	II	III
(A) Feb. 10-Mar. 9, 1947	5.0	3.0	1.4
(B) Mar. 22-Apr. 19, 1947	7.7	3.0	2.4
(C) 369 days from Jan. 6, 1947	0.7	2.7	0.1

In order to perform the test, it is necessary to know all the actual data unmanaged after the observation and calculate all the semi-amplitudes. But we have only the mean values in each lunar hour throughout one month (29 days) or one year (369 days) at hour hand. Therefore we treated the problem as follows for a preliminary trial.

We put N of $(N-2h-1)$ in the equation (2) as 24×29 in the case of one month and as 24×369, in the case of one year and calculated $\frac{1}{N}\sum u_t^2-\left(\frac{1}{N}\sum u_t\right)^2$ by means

* See for example, S.S. Wilks: Mathematical statistics, Chapter 8, Princeton University Press, 1943.

of 24 data (here $N=24$) and later multiplied it by 29 in the former case and by 369 in the later case in order to obtain.

The values of F_0 in the cases (A), (B) and (C) and $F^2_{N-2k-1}(\alpha)$ are given in the following table II.

Table II

	F_0	α (%)				
		0.1	1.0	5.0	10.0	20.0
(A)	2.9	6.91	4.64	3.01	2.30	1.61
(B)	1.4	6.91	4.64	3.01	2.30	1.61
(C)	11.35	6.91	4.60	2.99	2.30	1.61

In the case (A) 3 Km as the semi-amplitude of lunar semi-diurnal tide is significant with the level of significance of 10% and in the case (B) not significant even with 20%. In the case (C) it is significant with the level of 0.1%.

Judging from the considerations discussed in the preceding section and the data used, it is necessary to estimate the level of significance as a little higher than those listed in the table II. In the case (B) the level of significance will be heigher than 20% and in the case (A) the level of 10% may not be safe. Therefore it will be safe to consider the level of significance as more than 20% for both cases. But F_0 in the case (C) is sufficiently larger than 6.91 corresponding to the level of 0.1%, and it can be mentioned that the results of case (C) (2.7 Km) is significant with at least 1% of the significance level.

A doubt remains still on the significance of 2.7 Km as the semi-amplitude of lunar semi-diurnal tide, considering that it was an analyzed result by using the data observed with a fairly great scaling step of 10 Km. In the following section we investigate the problem of errors caused by scaling.

IV. Influence on a harmonic analysis caused by the errors attributable to scaling

1. Errors of a harmonic analysis

When we carry out a harmonic analysis, such as a periodgram analysis, by using $u(t)$, a periodgram h^2_N is given as follows,

$$h^2_N=\left[\frac{2}{N}\sum_{t=1}^{N}\{x(t)+\delta(t)\}\cos\lambda t\right]^2+\left[\frac{2}{N}\sum_{t=1}^{N}\{x(t)+\delta(t)\}\sin\lambda t\right]^2$$
$$=\frac{4}{N^2}[(\sum x\cos\lambda t)^2+(\sum x\sin\lambda t)^2]+Z^2 \qquad (4)$$

The first term in the above equation (4) is a periodgram in case of lacking error (δ), and this is the actual value we need. And Z^2 is the error of a periodgram which is attributable to δ. If we can mention with a large probability that Z is small enough in comparison with c_r in eq. (1), it must be recognized that the analysis using $u(t)$ is not senseless. Although we must know distribution of Z accurately for the estimation of Z, we try to estimate Z by calculating only $E(Z^2)$ or $E(Z^4)$ (E means average).

After comparing the various methods which can be employed the following one will be the most suitable for the present problem.

$$Pr\left(Z\leq\sqrt{\frac{1}{1-\varepsilon}E(Z^2)}\right)\geq\varepsilon \qquad (5)$$

The equation (5) shows the relationship between the minimum of the estimation of error (Z) and the given value of the lower limit of the confidence coefficient (ε). We neglect the equations corresponding to $E(Z^4)$ or the similar ones.

The calculated results of $E(Z^2)$ is

$$E(Z^2)=\frac{4}{N^2}\sum_{t=1}^{N}\{E[\delta^2(t)]+E[\delta(t)\,x(t)]\} \qquad (6)$$

2. Scaling and scaling skill (or carefulness)

We have to investigate the problem of scaling before we proceed forward. Though the minimum step of height scale is 10 Km in our case, it is generally put as k (Km).

i) The most skilful observer will record the height $u(t)$ as kp, when

$$kp-\frac{k}{2}\leqq x\leqq kp+\frac{k}{2} \qquad \begin{array}{l}(p:\ \text{integer})\\(x:\ \text{actual height})\end{array}$$

ii) In the case of very unskilful observer the probability with which he records the height $u(t)$ as kp will be equal to the probability with which he records $u(t)$ as $kp+k$ when $kp\leqq x\leqq kp+k$

That is

$$pr\,(u=kp)=pr(u=kp+k)=\frac{1}{2}$$

iii) But it is supposed that the actual cases will be intermediate between the above two situations.

This case is represented by

$$pr\,(u=kp)=\varphi\,(x),$$

where $\varphi(x)$ is an appropriate function of x, and we have to lay down the several conditions on $\varphi(x)$, considering the actual scaling practices. In general $\varphi(x)$ contains a few parameters which must be determined from the actual scaling. In the case of (i) and (ii) above mentioned, $\varphi(x)$ is the special cases without parameter, and also when $\varphi(x)$ is taken as of triangular shape, it is non-parametric. (See Fig. 1). In the following section we consider the two cases of (i) and the triangular shape.

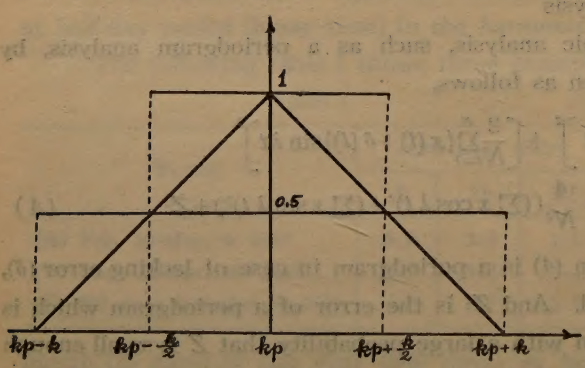

Fig. 1 A special case of $\varphi(x)$.

3. Calculation of $E(\delta^2)$ and $E(\delta x)$

In the case (i) mentioned above,

$$E(\delta^2)=\frac{k^2}{12}+\left(\frac{k}{\pi}\right)^2\sum_{n=1}^{\infty}(-1)^n\frac{1}{n^2}e^{-\frac{2n^2\pi^2\sigma^2}{k^2}}\cdot\cos\frac{2mn\pi}{k}$$

when m means an abbreviation of $m(t)$ in the equation (1), and σ^2 means the variance

of a random element $v(t)$.

Next we obtain the other equation $E(\delta x)$,

$$E(\delta x) = 2\sigma^2 \sum_{n=1}^{\infty} (-1)^n e^{-\frac{2n^2\pi^2\sigma^2}{k^2}} \cdot \cos \frac{2mn\pi}{k}$$

where k is the unit of scale and σ indicates the order of a variation. So it may be possible to assume as $k<\sigma$, and we can obtain the following results with a relative error smaller than 10^{-8},

$$E(\delta^2) = \frac{k^2}{12} \qquad (7)$$

$$E(\delta x) = 0 \qquad (8)$$

When the shape of $\varphi(x)$ is a triangle, we can obtain the results with errors of the same order as above,

$$E(\delta^2) = \frac{k^2}{6} \qquad (9)$$

$$E(\delta x) = 0 \qquad (10)$$

4. Estimation of Z

After substituting the pairs of equation (7), (8) and (9), (10) respectively in the equation (6), we get $E(Z^2)$ and then we calculate the equation (5) by using newly obtained $E(Z^2)$. The results are as follows.

In the case (i)

$$pr\left(Z \leq k\sqrt{\frac{1}{1-\varepsilon} \cdot \frac{1}{3N}}\right) \geq \varepsilon \qquad (11)$$

In the case, when the sharp of $\varphi(x)$ is a triangle,

$$pr\left(Z \leq k\sqrt{\frac{1}{1-\varepsilon} \cdot \frac{2}{3N}}\right) \geq \varepsilon \qquad (12)$$

By the ebuation (11) and (12), we calcurate the upper limit of Z corresponding to the lower limit of a confidence coefficient ε, putting $k=10$ Km, and get the results as shown in the following table III.

Table III

($k=$ 10Km)

Lower limit of a confidence coefficient (%)		99	95	90	80	70
an upper limit of Z of (i) (Km)	N=29×24	2.14	0.96	0.69	0.48	0.39
	N=369×24	0.62	0.27	0.19	0.04	0.03
an upper limit of Z when $\varphi(x)$ is a triangle (Km)	N=29×24	3.08	1.36	0.96	0.68	0.56
	N=369×24	0.86	0.38	0.27	0.06	0.05

According to the above table the error is very small in comparison with $c_r=$ 2.7 Km for the case of the analysis based on one year data ($N=369\times24$). For instance, when we take the confidence coefficient as 90%, we can consider the error as $Z\leq0.19$ (Km) in the case (i). The errors of such order will arrise as an error of analysis even if the scale is perfect. In the cases of $N=29\times24$, it is said that errors

will be fairly large even for the comparatively low coefficient of confidence as 80%.

V. Conclusions

We discussed about the significance and the error concerning the results of lunar tidal analyses of ionospheric height and described at first the test of statistical hypothesis as applied to some examples of harmonic analyses reported by Matsushita, assuming that the observed value $u(t)$ has Gaussian distribution $N(m(t), \sigma^2)$. Although $u(t)$ should be taken to deviate from this distribution owing to the scaling error, it is preferable to estimate the actual level of significance as larger to some extent than the calculated level based on normal distribution. Three examples of test for period of one month and one year for the lunar tidal analyses of ZmF_2 are presented.

Then we investigated errors, which are to be attributed to the scaling, that is, minimum step of ($k = 10$ Km) height mark and scalers skill (or carefulness) and presented some results of calculated errors.

The estimation of error (Z) is proportional to the width of scale (k) and inversely proportional to the square root of sample size (N) under some assumptions. In this connection the method of expressing the degree of skilfulness (or carefulness) of scaler was discussed.

The level of significance in the test of statistical hypothesis and the errors with a coefficient of confidence will serve as definite quantitative measures for criticizing the validity of the analyzed results.

Acknowledgements

The authors express their thanks to Mr. Matsushita for the kind cooperation with the materials and informations in his own work, and to members of the Ionosphere Research Committee for their valuable discussion.

References

(1) S. Chapman and J. Bartels: Geomagnetism, Oxford Press, 1940.

(2) K. Maeda and M. Izaki: Oral report at the monthly meeting of I.R.C. (Ionosphere Research Committee), Japan Science Council, Aug., 1950.

(3) S. Matsushita: On the Semi-diurnal lunar tide (M_2) in region F, J.G.G. Vol. 1, No. 1, p. 17, March 1949.

On the Charge Distribution in Volcanic Smoke

By G. ISHIKAWA,* M. KADENA* and M. MISAKI†

*Meteorological Research Institute, Tokyo and †Magnetic Observatory, Kakioka

Abstract

We made a simultaneous observation of the electric potential gradient and the space charge under the volcanic smoke of the new crater of Volcano Azuma in Fukushima-prefecture from August 13th to 19th 1950, to investigate the charge distribution in the volcanic smoke. The remarkable points which we obtained by the analysis of this observation are:

(i) The charge of the smoke of Volcano Azuma is positive, and the density of which is estimated at about 5 e.s.u./m^3 near the center of the smoke.

(ii) A thin layer of the negative charge is induced around the cylinder shaped smoke. The density of the induced charge is about 1/10 of that of the positive charge near the center of the smoke.

1. Introduction

Many investigations confirm the fact that the volcanic smoke has electric charge [1], [2], [3], [4], [5]. Most of these investigations, however, are conducted on the basis only of the electric potential gradient at the earth's surface under the smoke, so that it is inevitable that an arbitrariness should enter into the deduction of charge distribution in the smoke. For example, even if the variation of the electric field under the smoke is negative, we cannot say that there is no region of positive charge in the smoke.

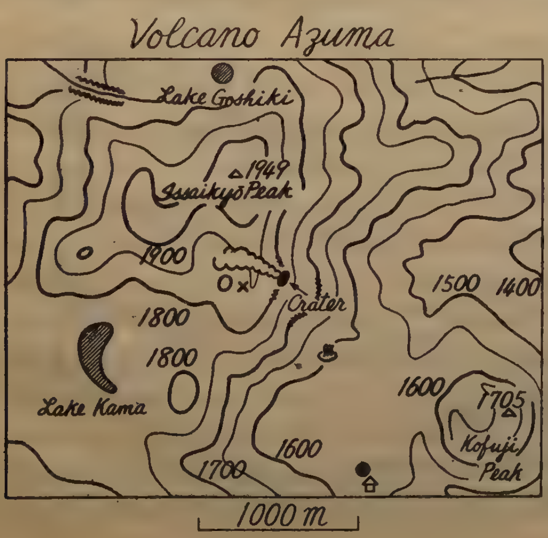

To confirm the charge distribution more in detail we must carry out the simultaneous observation of the potential gradient and the space charge, which we made actually at Volcano Azuma. Volcano Azuma had been dormant until the recent eruption on Feb. 10th, 1950, since the last eruption of 1896. The recent eruption occurred without any symptom, followed by a second smaller one on the 19th of the

same month. It was observed that large quantities of ashes, pieces of lava and rocks were scattered as far as 600 meters from the crater. When we made the observation there, Volcano Azuma was already in a quiet condition as before. Its smoke was white, looked like a steamjet, and was supposed to contain a very small amount of solid particles. The state in such smoke must be greatly different from that in black smoke. The observing point O was in the leeward of the crater and the smoke flowed over it almost continuously, and frequently it came down to the surface of the slope, covering the observing instruments. The smoke remained in general the circular

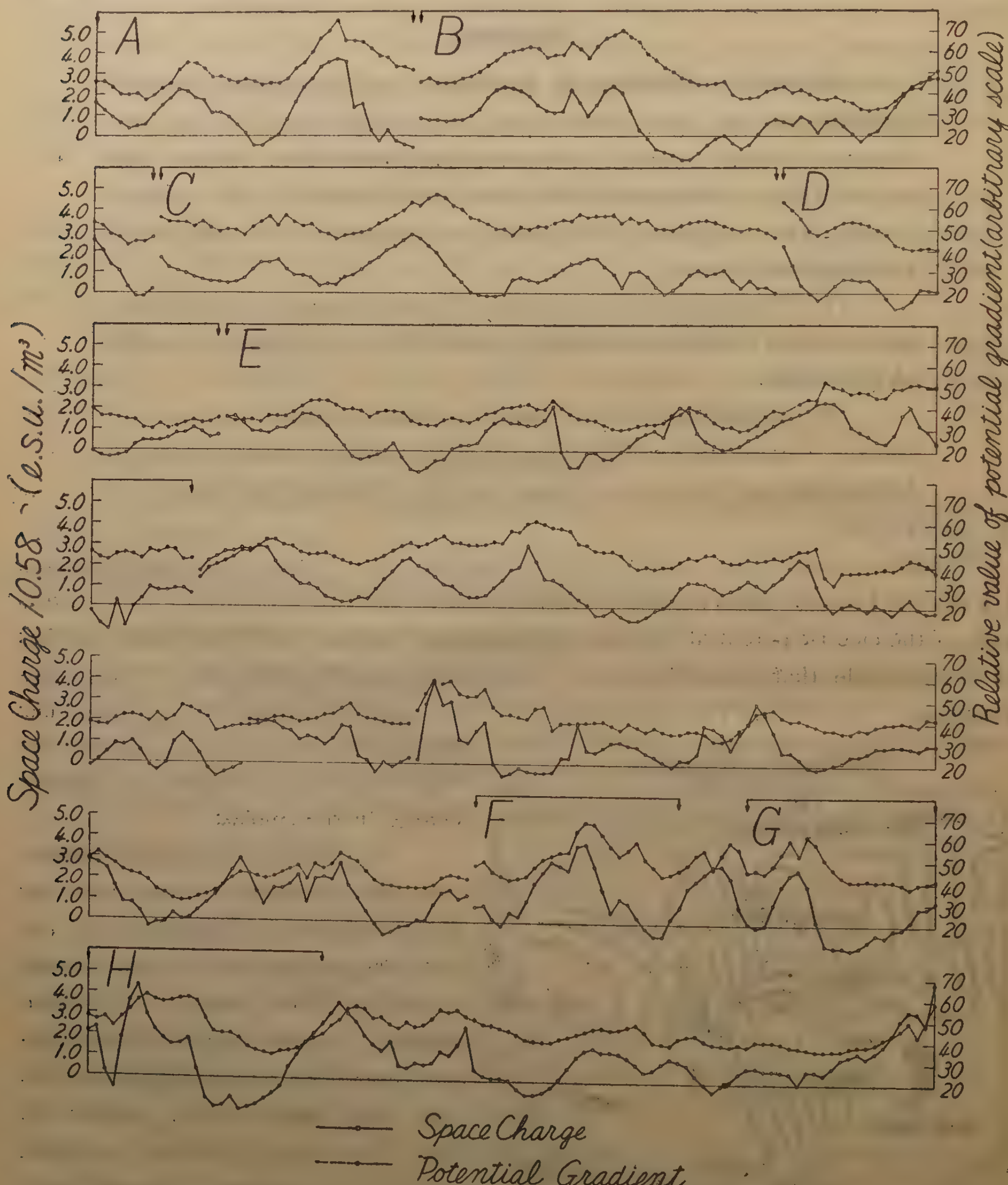

Fig. 2 Samples of the results of simultaneous observation of the space charge and the potential gradient.

cylinder shape, whose diameter was estimated to be about 30 to 50 meters, except when it swept down to the ground.

2. Observing Instruments and the Results Obtained

The instrument used in measuring the electric field is the portable electrometer with a radioactive collector mounted on a tripod. Owing to the rocky, complex configuration of the ground, it is difficult to make plane reduction for the observed values of the potential gradient. Since the position of the electrometer relative to the circumstances was not changed during the observation, the observed value is regarded as the relative value of the electric field at the point O. The instrument used for mesuring the space charge is a cubic brass cage, whose side is 90 centimeters long, and at the center of which a radioactive collector was held by a bamboo rod. The scale value of this instrument is,

$$\rho = 0.58\ V \text{ e.s.u./m}^3$$

where V is the electric potential of the collector measured in volt.

Among the results observed, the most reliable values at point O are inserted in Fig. 2. On seeing this, it is evident first that the electric field under the smoke is always positive and also the space charge is almost always positive except in the short durations in which it has a small negative value. Secondly, the variation of the electric field and the space charge are parallel. For example, dividing the data into the groups A, B, C, D and E, as shown in Fig. 2, we obtain the correlation coefficients between the electric field and the space charge in each group, which are,

Group	Sample number	Correlation coefficient
A	39	0.56
B	70	0.46
C	74	0.63
D	35	0.22
E	98	0.39

In groups A, B and C, a good positive correlation is observed, but not so in groups D and E. However, the electric field strength and the space charge have a similar tendency in small variation, even in groups D and E, only a linear relation between them is partly broken, owing to the superposition of large variations, which are not related linearly to each other. We notice thirdly that the positive maximum values of the space charge fluctuate pretty largely but its negative minimum values remain fairly constant, that is, near 0.5 e.s.u./m^3. Further, it is remarkable that the space charge was generally in inverse proportion to the distance from the center of the smoke, and that the distance where the space charge changes from positive to negative, is found to be about 60 meters, as shown in Fig. 7. The distance between the center of the smoke and the observing point is estimated with eye-observation. In practice, the horizontal and vertical distances (X, Z) were observed with respect to a co-ordinate, having an origin at the observing point and the X-Z plane being at

right angles to the center line of the smoke cylinder. The eye-observation of the distance may have an error of ± 10 meters.

3. Charge Distribution In and Around the Smoke

On the basis of the observed data stated above, we consider the charge distribution in the smoke. It must be noted first that, since the electric field is always positive at the ground surface, the main part of the smoke may be expected to have positive charge. The intensity of the field strength is estimated ten times as large as the ordinary value, considering the sensitivity of the electrometer and its relative position to the surroundings. The observed value of the space charge frequently became 3 e.s.u./m³. The smoke remains in general the shape of circular cylinder without being broken to pieces. Taking these facts into consideration we may assume that the charge density of the smoke ρ_0 has the following expression,

$$\left.\begin{aligned} \rho_0(r) &= \rho_m\left(e^{-\frac{r^2}{2\sigma^2}} - e^{-\frac{a^2}{2\sigma^2}}\right) & r<a \\ &= 0 & r>a \end{aligned}\right\} \tag{1}$$

where r is the distance from the center of the smoke cylinder, and ρ_m, σ and a are constants which are estimated respectively,

$$\rho_m = 5\ \text{e.s.u./m}^3, \qquad \sigma = 25\ \text{m}, \qquad a = 70\ \text{m}.$$

The space charge ρ, which is actually observed, is the sum of ρ_0 and the charge induced by the smoke. Since the mobility of the smoke particle is considered as smaller than that of a large ion, ρ_0 may be assumed to be constant within a comparatively short time after the smoke starts from the crater. The distance between the crater and observing point is about 350 meters and the wind velocity was about 3 meter/sec. during the observation, so the smoke takes about two minutes on the average to travel over the distance from the crater to the observing point. Fig. 3 shows schematically the aspect of the inducing negative charge around the smoke.

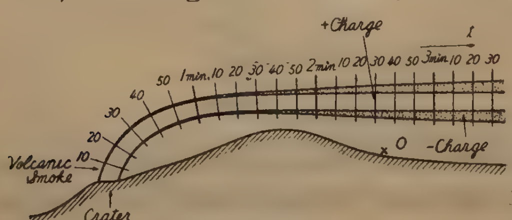

Fig. 3 : The schematic aspect of the inducing negative charge around the smoke.

The charge quantity per meter along the smoke cylinder is calculated as,

$$Q = \int_0^a \rho_0(r)\cdot 2\pi r dr = 177\ \text{e.s.u./cm} = 5.9\times 10^{-8}\ \text{coulomb/cm} \tag{2}$$

The electric field in and outside the smoke becomes,

$$\left.\begin{aligned} E_0(r) &= \frac{2\pi\rho_m}{r}\left[2\sigma^2\left(1-e^{-\frac{r^2}{2\sigma^2}}\right) - r^2 e^{-\frac{a^2}{2\sigma^2}}\right] & r<a \\ &= 2Q/r & r>a \end{aligned}\right\} \tag{3}$$

The charge distribution ρ_0 and the electric field E_0 in the initial state are shown in Fig. 4. For example, if this smoke has a length of 10 km, the total charge in it

becomes about 0.06 coulombs and is one or two orders less than that expected on Volcano Asama and Volcano Yake. It may be natural, since the smoke of Volcano Azuma is fairly weaker than that of the above two mountains. Now assume that the positive and negative ions are spread homogeneously in the nitial state outside the smoke, then the positive ions move in the direction of r. Let us consider first the motion of a positive charge outside the smoke. Using the equation (3), we have,

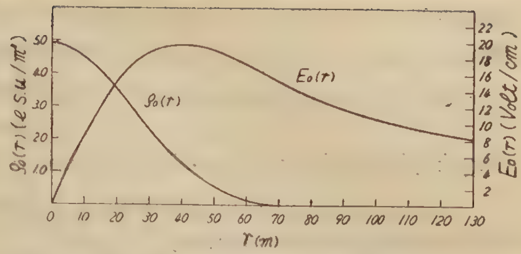

Fig. 4 : The space charge ρ_0 and the electric field intensity E_0 of the smoke in the initial state.

$$dr^+/dt = kE_0 = 2kCQ/r^+, \qquad r^+ > a \tag{4}$$

where Q is measured in practical unit and C is a constant, having a value of 9×10^{11}. Integrating the above equation we obtain,

$$r^+ = (4\,kC\,Q\,t + s^2)^{\frac{1}{2}} \tag{5}$$

where s is the position of the ion considered at the initial state. From this, we get,

$$dr^+/ds = s/r^+. \tag{6}$$

So that,

$$[\rho^+(k)\,dk]_{t=t} = [\varepsilon\,f(k)\,dk]_{t=t} = [\rho^+(k)\,dk]_{t=0} = \text{const.} \tag{7}$$

is valid in the region, in which the positive charge of mobility k can exist. Here,

ε : the charge of an ion

$f(k)\,dk$: spectral density function of positive ion, whose mobility is between k and $k+dk$.

Consequently, the charge density with only positive ions at a certain place and time becomes,

$$\rho^+(r,t) = \varepsilon\int_0^{\underline{k}} f(k)\,dk \tag{8}$$

where,

$$\underline{k} = \frac{r^2-a^2}{4CQt} \tag{9}$$

On the other hand, the charge density with negative charges alone becomes,

$$\rho^-(r,t) = -\varepsilon\int_0^{\infty} f(k)\,dk \tag{10}$$

assuming that the mobility spectrum of the negative ion is the same to that of the positive one. Therefore the total charge density outside the smoke is,

$$\rho(r,t) = -\varepsilon\int_{\underline{k}}^{\infty} f(k)\,dk \qquad r>a \tag{11}$$

The field $E_0(r)$ is scarcely modified by the induced charges, owing to its small quantity compared with ρ_0. We adopt the approximate form for the mobility spectrum of the ion, referring to Misaki's results [6], which gives,

$$f(k)\,dk = \sum_{i=1}^{3} A_i \exp\left\{-\frac{(X-\mu_i)^2}{2\nu_i^2}\right\}dX \tag{12}$$

where, $X = \log k$,

and $i = 1$: small ion

2: intermediate ion

3: large ion.

For simplicity, let us consider the case $i=1$,

$$A_1 = 334, \qquad \mu_1 = o, \qquad \nu_1 = 0.458.$$

In this case $f(k)\,dk$ becomes,

$$\left.\begin{aligned} f(k)\,dk &= 216 \exp(-\xi^2)\,d\xi \\ \xi &= 1.543 \log k \end{aligned}\right\} \tag{13}$$

Making use of the above density function we obtain,

$$\rho(r,t) = -3.07\times10^{-17}\left\{1-\frac{2}{\sqrt{\pi}}\int_0^{\xi} e^{-\xi^2}\,d\xi\right\} \qquad r>a \tag{14}$$

where,

$$\xi = 1.543 \log\left\{\frac{r^2-a^2}{2.12\times10^5 t}\right\}$$

Next, we must consider the case $r<a$. We found easily, however, that the charge distribution of the negative ion inside the smoke is identical with that outside the smoke in the first approximation, after a simple calculation similar to the case of outside the smoke. Thus we have,

$$\rho(r,t) = \rho_0(r) - 3.07\times10^{-17} \times\left\{1-\frac{2}{\sqrt{\pi}}\int_0^{\xi} e^{-\xi^2}\,d\xi\right\} \quad r<a \tag{15}$$

Fig. 5 is calculated by the above formulae for the various r's and t's. Similar calculation is also valid for the case of large or intermediate ions. The charge density, however, calculated from the equations (14) and (15), is too small to explain the observed results. So that for explaining the actual results quantitatively, we have to adopt a more larger value of A_1 than that obtained at the ordinary

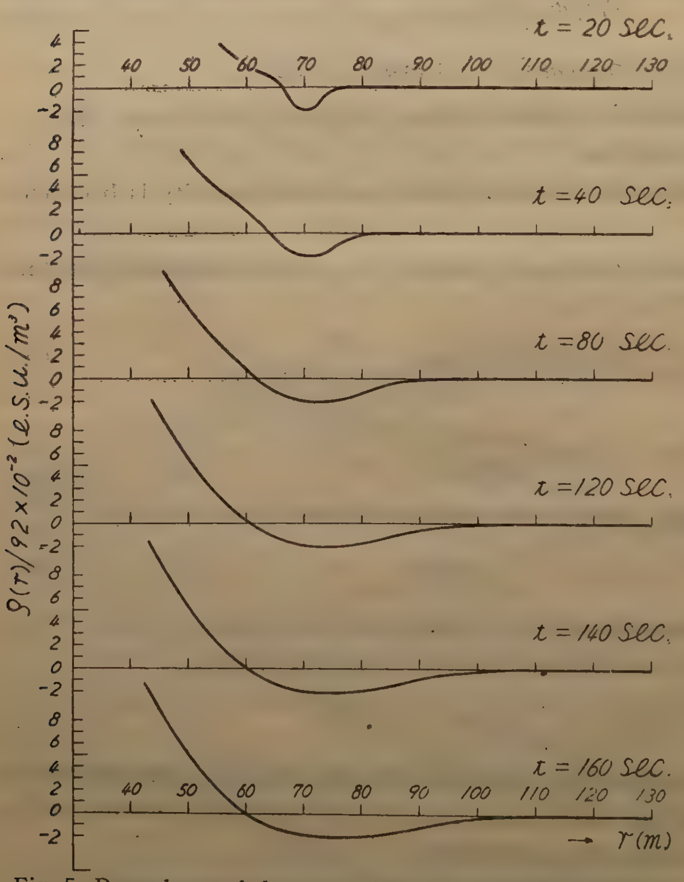

Fig. 5 Dependence of the space charge around the smoke and the distance r for the various t's.

place. To consider the cases where $i=2$ or 3 will also serve to enlarge the density of induced negative charge. Next we consider the electric field under the smoke. Taking the image charge against the earth's surface into consideration, the electric field on the ground surface is given by,

$$Ex=0, \quad Ez=-(4ZCQ)/R^2 \quad \text{Volt/cm}$$

where,

$$R^2=X^2+Z^2 \qquad (16)$$

is the distance between the center of the smoke and the observing point. Using meter for the unit of length, we can rewrite the above equations as,

$$Ez=-2120\, Z/R^2 \quad \text{Volt/cm} \qquad (17)$$

The electric field calculated with the above equation is shown in Fig. 6.

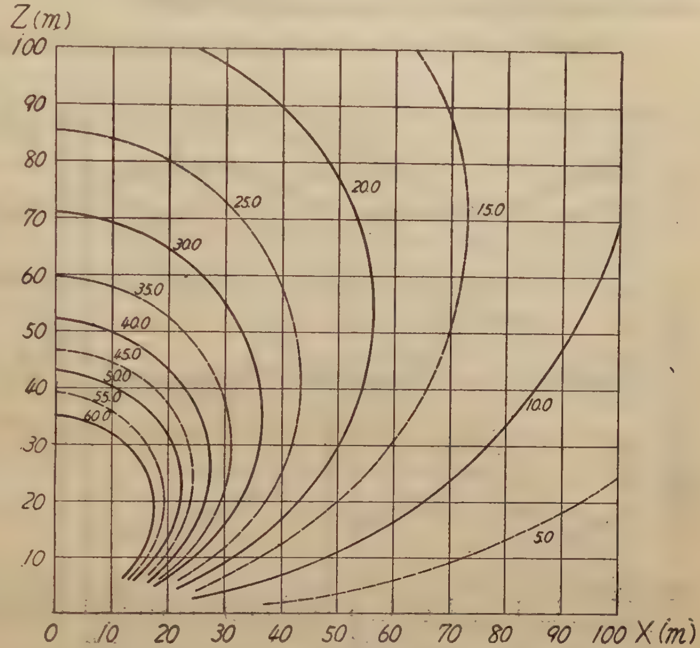

Fig. 6: The contour line showing the position of the center of the smoke which gives the same electric field intensity at the origin (The value on the contour shows the electric field intensity at the origin measured in volt/cm).

4. Discussion

We shall examine how the charge distribution obtained in the previous section will explain the observed results. From Fig. 5, it is expected that, as the center of the smoke moves, the maximum value of the space charge considerably fluctuates in the positive region, but in the case of negative region, its minimum value may have an almost constant value. Since Fig. 5 is that calculated only for the small ion, the effects of the intermediate and the large ion must be taken into account. The calculated value of $\rho(r)$ in the case that the effect of the intermediate ion is considered, is illustrated in Fig. 8. The depth of the channel of negative charge around the smoke is determined by the shape of the ion spectrum. It is likely in the actual case that the steplike part of the charge distribution in Fig. 8 will be made more smooth by the turbulence of the wind. In either case, the depth of the channel of negative charge around the smoke may be nearly constant within a comparatively short space of time. The problem we must consider next is whether we are justified in neglecting the effect of the ground in equation (4). We may approximate it more closely, using the equation (17) instead of (3). Speaking qualitatively, to make use of the equation (17) results in broadening the width of the channel of negative charge just under the smoke twice as large as that just above it. In the actual case, however, $\rho_0(r)$ will be distorted considerably as the smoke approaches to the ground, so

that detailed calculation with the equation (17) may be rather insignificant.

As a transient case we introduced the equations (14) and (15), that is, we entirely neglected the recombination of the ions. But, if we consider it, the result obtained may not be modified so largely in this case because the time after the smoke starts from the crater is comparatively short.

Though it is such a rough approximation, the charge distribution obtained

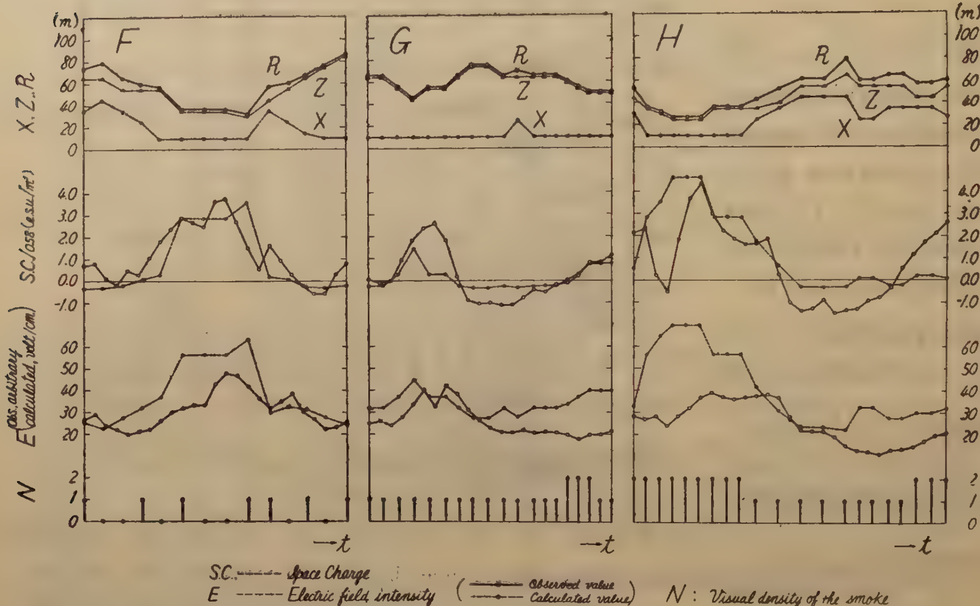

Fig. 7 : The comparison of the calculated values of space charge and the potential gradient with those of the observed values.

above can explain the various phenomena shown in the second section. From the equations (15), (16) and (17) it is clear that the variation of the space charge and that of the electric field strength are almost parallel to each other, both inversely proportionate to R. The values of ρ and E obtained from actual observation and those by calculation in which the case $t=140$ sec. is adopted, are illustrated in Fig. 7. So far as the smoke does not approach very near to the observing point, the calculated values sufficiently coincide with the observed values. Further, the smoke often changed its density, the state of which is roughly shown in Fig. 7, and the wind velocity was not always constant, therefore the width of the channel of negative charge is naturally expected to fluctuate, but a detailed discussion of such effects is beyond our present treatment.

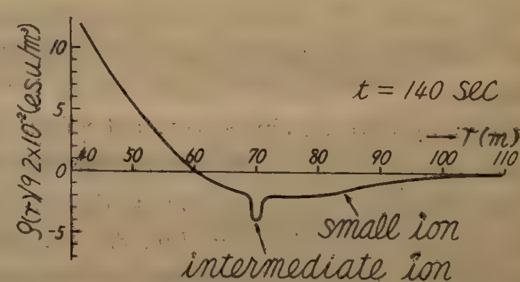

Fig. 8 : The curve of $\rho(r)$ in the case that both small and intermediate ion are considered.

We should like to express our hearty thanks to the members of the staff of the

Fukushima Meteorological Station for their great help in this observation and also to Dr. H. Hatakeyama, Director of the Meteorological Research Institute, for his kind suggestion and encouragement in the present research.

References

[1] H. Hatakeyama: Journ. Met. Soc. Japan, **21**, 49, 420, 426 (1943).

[2] K. Hirao and Others: Geophys. Notes, No. 28, 25 (1947).

[3] H. Hatakeyama: Journ. Met. Soc. Japan, **25**, 39 (1947).

[4] H. Hatakeyama: Journ. Geomag. and Geoelectricity, **1**, No. 2, 48 (1949).

[5] H. Hatakeyama and K. Uchikawa: Papers in Met. and Geophys., **2**, No. 1, 85 (1951).

[6] M. Misaki: Papers in Met. and Geophys., **1**, No. 2–4, 313 (1950).

The Annual- and Diurnal Variations of Cosmic-Ray Intentsity and the Temperature Effect

By Kaichi MAEDA and Tomoshige SUDA

Meteorological Research Institute, Tokyo

Abstract

In order to estimate the influence of the diurnal variation of the atmospheric temperature on that of cosmic ray intensity, we investigated the bihourly data of cosmic ray intensity at Huancayo and aerological data at San Juan. As the mean atmospheric temperature, the altitude differences between 100 mb. and 1000 mb. levels were used. We ascertained that the amplitude of the diurnal change of cosmic-ray intensity at Huancayo exceeded 0.5% at least (i.e. twice that of the observed value), if the temperature effect was taken into accounts.

1. Introduction.

Previously, we disccussed in brief (1) the influence of the diurnal variation of mean atmospheric temperature upon that of cosmic ray. The upper-air data used in that discussion, however, were not accurate enough to treat of such a problem quantitatively. Therefore, we have investigated on this problem with respect to the cosmic ray data of Huancayo, taking reliable aerological data of the diurnal change into accounts. In this paper, the temperature effect is regarded as the decay effect of meson component produced in the layer of about 100 mb. level, so that the coefficient of this effect is represented by the variation of cosmic ray intensity in % per altitude difference between 100 mb. and 1000 mb. levels in km.

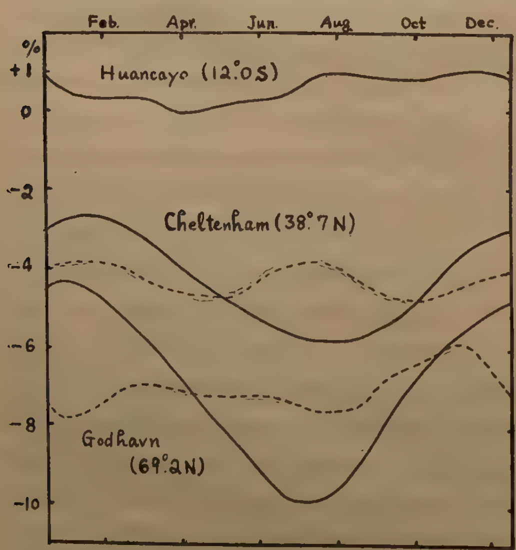

Fig. 1 The Annual Variation of Cosmic-Ray Intensity.

2. The Annual Variation of Cosmic Ray.

Fig. 1 shows the curves of annual variation of cosmic ray intensity at Huancayo (12.°0 S), Cheltenham (38.°7 N) and Godhavn (69.°2N) which denote the averaged values of five years from 1939 to taken 1944, from the monthly data (2). It is clear that the amplitudes are larger in

high latitudes than in low, and this is of course due to the so-called temperature effect ont he cosmic ray. Therefore, in order to estimate the coefficients of this effect for these data, the annual variations of the altitude difference between 100 mb. and 1000 mb. levels at Swan Island (15° N), San Juan (17° N), Washington (38.°9 N) and Thule (77 °N) are evaluated as in Fig. 2. The curves are computed from the daily upper air data published by Weather Bureau, U.S.A. in 1950.

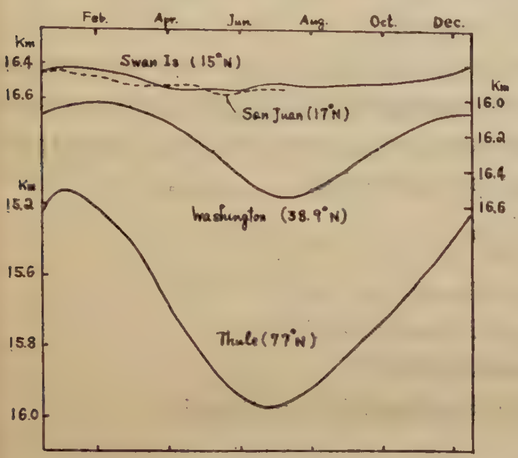

Fig. 2 The Annual Variation of the Altitude Difference between 100mb. and 1000mb. Levels.

As a rough estimation of the coefficients, taking the ratio of both these amplitudes, it follows

–9.0%/km for Huancayo
–5.5%/km for Cheltenham
and –3.4%/km for Godhavn.

Among these values, –5.5%/km is only plausible because Washington and Cheltenham are very nearly situated and no complete upper air soundings for the year are available except for Washington. Moreover, the value –5.5 %/km is exactly the same with that determined by the calculation of regression coefficient. Dashed lines in Fig. 1 denote the curves corrected by these coefficients using the curves in Fig. 2. In the corrected curves, the semi-annual changes are predominant, but this is merely apparent because both data are taken from different years.

3. The Diurnal Variation of Cosmic-Ray Corrected for the Temperature Effect.

In order to consider the temperature correction which affects the forms of the diurnal variation of cosmic ray intensity at Huancayo, the diurnal variation of the altitude difference between 100 mb. and 680 mb. levels is calculated as the lowest curves in Fig. 3 from the data of three-hour interval observations by radio-sonde performed at San Juan during October and November in 1944, for the data of Huancayo are corrected to the values of 510 mmHg (i.e. 680 mb) for the pressure effect. Usually the day-time temperature in upper atmosphere is overestimated owing to the solar heating of meassuring instruments and this gives an enlarged amplitude

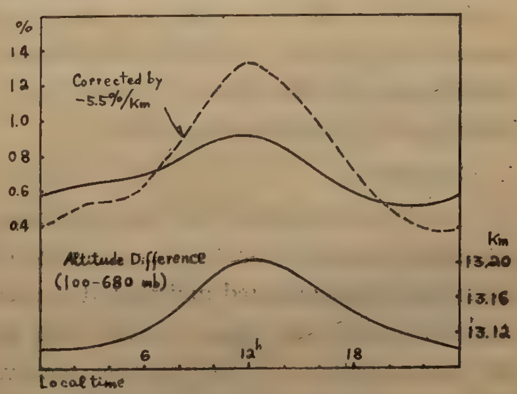

Fig. 3 The Diurnal Variation of the Cosmic-Ray (upper) and the Altitude Differnce between 100mb and 680mb Levels (below).

of the diurnal changes of the isobar heights in the upper atmosphere. But, in this respect, those results are corrected cautiously by the graphical method (3) and per-

mit us to use them for our purpose because the diunal variations of aerological states may be regarded to be similar in San Juan and Huancayo though they are in a difference hemisphere from each other.

Now, to estimate the temperature effect for the date of Huancayo, let us consider the altitude dependency of cosmic ray intensity in the lower atmosphere simply as

$$I=I_0 \exp\{-\beta(h-z)\}$$

where I is the intensity at the height z km above the sea level, I_0 is the intensity at the meson producing layer whose height is assumed to be h km above the sea level, and β is the mean decay coefficient of the meson component and this is equal to the reciprocal of L, the mean life range, wlich is expressed by

$$\mathrm{L}=\frac{\tau_0}{m_0}p$$

if we indicate by τ_0, the life time of meson (nearly 2μ sec.),

by m_0, the rest mass of meson (nearly 10^8 eV/c^2)

and by p, the momentum of meson in MeV/c.

Then the coefficient of temperature effect at sea level, b, is written by

$$b=\frac{1}{I}\frac{\partial I}{\partial h}\bigg|_{z=0}=-1/\mathrm{L}$$

and at the height of z

$$b'=\frac{1}{I}\frac{\partial I}{\partial h}\bigg|_{z=Z}=-1/\mathrm{L}'$$

Thus, we get

$$b'=\frac{\mathrm{L}}{\mathrm{L}'}b$$

where L and L$'$ represent the mean life range at $z=0$ and $z=Z$ respectively and according to Bennedetto (4) L$\doteqdot$14.2 km (this corresponds to $p=2.7\times10^3$ MeV/c). It is clear that L$'$ is shorter than L, for the momentum spectrum increases with the altitude more rapidly in lower regions than in higher. Put L$'$=8.7 km (this corresponds to $p=1.7\times10^3$ MeV/c), then we get $b'=-9.0\%$/km as shown above, but this value seems to be too large, so that as the lowest estimation we take -5.5%/km. The corrected curves by this factor is shown in Fig. 3 by the dotted line, while the full line indicates the uncorrected variation.

4. Conclusion.

It is not deniable that the amplitude of the diurmal variation of cosmic ray intensity corrected for the temperature effect at Huancayo becomes at least nearly twice that of uncorrected and that it exceeds 0.5% at noon. Although our investigations as regards the data of middle and high latitudes are not sufficient, owing to the incompleteness in the reliable observations of diurnal variation in the upper atmosphere, we may conclude that the temperature effect is not negligible for the discussion of the diurnal variation of cosmic ray intensity. Finally some of the origins of these diurnal changes might be expected in the upper air state as pointed by Duperier (5) and Rathgeber (6). In this respect more accurate knowledge of the upper atmosphere is needed.

Our thanks are due to Dr. K. Takahashi, Forecast Research Laboratory of this Institute, for his kind informations about aerological data.

References

(1) K. Maeda; T. Suda: Report of Ionos. Res. in Japan **5** No. 2 (1951).

(2) Cosmic Ray Results from Huancayo Observatory, Peru June 1936 December 1946.

(3) H. Riehl: Amer. Met. Soc. **28**, 311 (1947).

(4) F.A. Benedetto: Phys. Rev. **70**, 817 (1946).

(5) A. Duperier: Proc. Roy. Soc. A **62**, 687 (1949), Nature. **167**, 312 (1950).

(6) H.D. Rathgeber: Proc. Phys. Soc. **63**, 368 (1950).

LETTER TO EDITOR

A Newly Designed Differential Electrometer and its Application to the Simultaneous Measurment of Air Earth Current and Potential Gradient

F.J. Scrase[1] made a simultaneous measurement of air earth current and atmospheric potential gradient using radioactive collector and Wilson's test plate. In order to eliminate the induced charge on the test plate due to atmospheric electric field and to get pure air earth current, Scrase employed the quadrant electrometer differentially. In this case the electric potentials on each two quadrants are same sign, so that by suitable adjustment two potentials are compensated each other, and the electrometer is being charged by pure air earth current only. When the sign of two potentials, which are to be compared each other, are opposite, we can not use quadrant electrometer differentially. For this purpose new type of differential electrometer becomes neccessary. This new electrometer is designed and constructed by the author.

The principal parts of the electrometer consist of, as shown in Fig. I a, two needles fixed perpendicularly each other to the metal stick, on which a small mirror

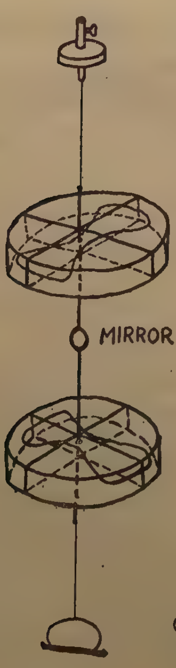

Fig. 1 a

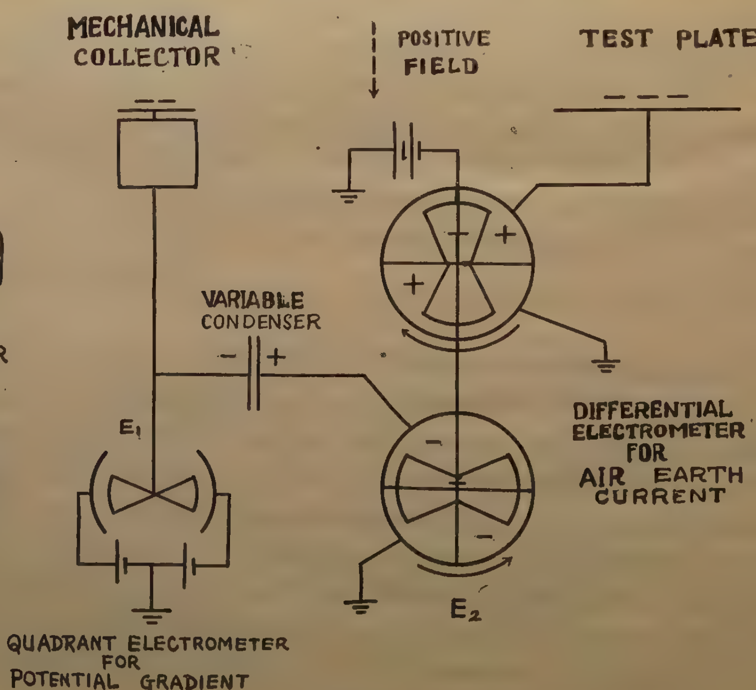

Fig. 1 b

is attached at the middle point, and the double quadrant system are located above and below. As an example, the author applies this electrometer to the simultaneous measurements of air earth current and potential gradient using rotating collector and test plate. In the case of this collector, rotating vane is earthed when exposed to the atmospheric electric field, and connected to the electrometer when covered by the earthed shield, so that the sign of the potential obtained is negative when the atmospheric electric field is positive, or vis-versa.

Fig. I b shows the connection circuit. The electrometer E_2 should be deflected by the charge accumulated by the air earth current flows into the test plate. The charge induced on the test plate by the atmospheric electric field is compensated by the action of rotating collector through variable condenser adjusted suitably. In this figure the manner of compensation is shown in the case of atmospheric field is positive. We can find the fine structure between air earth current and potential gradient by this method. Employing such a electrometer some measurements were carried out. The detailed results of this measurements will be reported in the near future.

The author expresses his thanks to Dr. Prof. M. Hasegawa and Dr. Y. Tamura for their valuable advices.

By Miyoji Goto

Aso Magnetic Observatory, Kyoto University

---

(1) F.J. Scrase, Geophys. Mem., No. 58, 1933.

昭和26年10月25日 印刷
昭和26年10月31日 發行
第3卷第1號　定價150圓
（國外定價180圓）

編輯兼發行者　日本地球電氣磁氣學會
代表者　長　谷　川　万　吉

印刷者　京都市下京區上鳥羽學校前
田　中　幾　治　郎

賣捌所　丸　善　株　式　會　社　京　都　支　店
丸善株式會社　東京・大阪・名古屋・仙台・福岡

JOURNAL OF GEOMAGNETISM AND GEOELECTRICITY

Vol. III No. 1

1 9 5 1

CONTENTS